Journal of Hematology & Oncology

RESEARCH

Open Access

IL1RAP-specific T cell engager depletes acute myeloid leukemia stem cells

Yi Zhang[1,2†], Miso Park[3†], Lucy Y. Ghoda[2†], Dandan Zhao[2], Melissa Valerio[2], Ebtesam Nafie[2], Asaul Gonzalez[3], Kevin Ly[3], Bea Parcutela[3], Hyeran Choi[3], Xubo Gong[2,4], Fang Chen[2], Kaito Harada[2], Zhenhua Chen[5], Le Xuan Truong Nguyen[2], Flavia Pichiorri[2], Jianjun Chen[5], Joo Song[6], Stephen J. Forman[7], Idoroenyi Amanam[2], Bin Zhang[2*], Jie Jin[1*], John C. Williams[3*] and Guido Marcucci[2,7*]

Abstract

Background The interleukin-1 receptor accessory protein (IL1RAP) is highly expressed on acute myeloid leukemia (AML) bulk blasts and leukemic stem cells (LSCs), but not on normal hematopoietic stem cells (HSCs), providing an opportunity to target and eliminate the disease, while sparing normal hematopoiesis. Herein, we report the activity of BIF002, a novel anti-IL1RAP/CD3 T cell engager (TCE) in AML.

Methods Antibodies to IL1RAP were isolated from CD138+ B cells collected from the immunized mice by opto-electric positioning and single cell sequencing. Individual mouse monoclonal antibodies (mAbs) were produced and characterized, from which we generated BIF002, an anti-human IL1RAP/CD3 TCE using Fab arm exchange. Mutations in human IgG1 Fc were introduced to reduce FcγR binding. The antileukemic activity of BIF002 was characterized in vitro and in vivo using multiple cell lines and patient derived AML samples.

Results IL1RAP was found to be highly expressed on most human AML cell lines and primary blasts, including CD34+ LSC-enriched subpopulation from patients with both de novo and relapsed/refractory (R/R) leukemia, but not on normal HSCs. In co-culture of T cells from healthy donors and IL1RAP^{high} AML cell lines and primary blasts, BIF002 induced dose- and effector-to-target (E:T) ratio-dependent T cell activation and leukemic cell lysis at subnanomolar concentrations. BIF002 administered intravenously along with human T cells led to depletion of leukemic cells, and significantly prolonged survival of IL1RAP^{high} MOLM13 or AML patient-derived xenografts with no off-target side effects, compared to controls. Of note, BiF002 effectively redirects T cells to eliminate LSCs, as evidenced by the absence of disease initiation in secondary recipients of bone marrow (BM) from BIF002+T cells-treated donors (median survival not reached;

Presented in oral form at the 65th annual meeting of the American Society of Hematology; San Diego, CA, 10 December 2023.

†Yi Zhang, Miso Park and Lucy Y. Ghoda have contributed equally to this study.

*Correspondence:
Bin Zhang
bzhang@coh.org
Jie Jin
jiej0503@zju.edu.cn
John C. Williams
jcwilliams@coh.org
Guido Marcucci
gmarcucci@coh.org
Full list of author information is available at the end of the article

all survived > 200 days) compared with recipients of BM from vehicle- (median survival: 26 days; $p = 0.0004$) or isotype control antibody+T cells-treated donors (26 days; $p = 0.0002$).

Conclusions The novel anti-IL1RAP/CD3 TCE, BIF002, eradicates LSCs and significantly prolongs survival of AML xenografts, representing a promising, novel treatment for AML.

Keywords IL1RAP, T cell engager, Acute myeloid leukemia, Leukemic stem cells, Immunotherapy

Background

Acute myeloid leukemia (AML) is a cytogenetically and molecularly heterogeneous clonal disease characterized by the accumulation of undifferentiated leukemic cells (blasts), which culminates in bone marrow (BM) failure [1]. Despite newly approved drugs, the 5-year overall survival (OS) of AML patients remains only ~ 30% [2–4]. The persistence of leukemic stem cells (LSCs), a highly treatment-resistant set of primitive cells capable of unlimited self-renewal and of disease initiation and maintenance, is recognized as one of the root causes of treatment failures in AML patients [5–7]. While allogenic hematopoietic stem cell transplantation can effectively eliminate LSCs through a graft-vs-leukemia effect and in turn achieve a cure, its applicability is limited to healthier and younger AML patients. Thus, more effective, and safer therapies are urgently needed.

Recently, immune checkpoint inhibitors, monoclonal antibodies, bispecific T cell engager antibodies (TCEs), and chimeric antigen receptor T cells (CAR-T cells) have emerged as novel immune-based approaches for cancer treatment [8–11]. While these approaches have been successfully applied to B lymphoid leukemias, they are still under investigation for AML. TCEs incorporating anti-CD3 and targeting CD33, CD123, CLL-1 and FLT3 as well as CAR-T cells targeting CD123 and CD33 are currently being tested in clinical trials for AML, but to date none of them has been approved [12–19]. Of note, CD33, CD123, and CLL-1 are variably expressed on normal CD34+ hematopoietic stem and progenitor cells (HSPCs) [20–23], raising concerns for intrinsic TCE on-target, off-leukemia hematologic toxicity.

The interleukin 1 receptor accessory protein (IL1RAP) is a member of the IL-1 superfamily and is expressed in the liver, placenta, and white blood cells (NCBI Gene ID 3556; UniProtKB ID Q9NPH3; Bgee Gene ID ENSG00000196083). It has also recently emerged as a therapeutic target for AML and solid tumors [24, 25]. IL1RAP plays a central role in amplification and transmission not only of the signals and activity of IL-1 family of cytokines, including IL-1, IL-33, IL-36, but also of other membrane proteins including tyrosine kinase receptors, e.g., Fms related receptor tyrosine kinase 3 (FLT3) and C-kit, and cystine transporters [26–29]. Of note, IL1RAP is reportedly highly expressed on the surface of AML, chronic myeloid leukemia (CML) and high risk-myelodysplastic syndrome (MDS) cells and associated with rapid disease progression and poor outcomes [30, 31]. Importantly, IL1RAP is expressed at significantly lower levels in normal HSCs compared with AML LSCs, and therefore it may represent an ideal immunotherapeutic target [32, 33]. To this end, blocking IL-1 signaling with IL-1 receptor antagonists [34] or a monoclonal antibody, has resulted in inhibition of leukemia growth, without effects on normal hematopoiesis [25, 32, 35]. Currently, monoclonal IL1RAP antibodies are being tested in clinical trials of both solid tumor and leukemia patients [36]. IL1RAP CAR-T cells have also demonstrated activity in preclinical models and are being tested in the clinic [37, 38]. However, to our knowledge, IL1RAP TCEs have not yet been reported.

Herein, we describe the development and functional characterization of BIF002, a novel anti-IL1RAP/CD3 TCE. Fab arm exchange was used to create an IgG-like molecule with high affinity to human(h) IL1RAP and relatively weak affinity to CD3. Mutations in the Fc were incorporated to reduce FcγR binding. We observed significant preclinical activity of BIF002, with no evidence of interference with normal hematopoiesis or non-hematologic toxicities. Importantly, using AML patient-derived xenografts (PDXs), in secondary transplant experiments, we showed that BIF002 was able to eliminate LSCs.

Methods

Generation of BIF002 and controls

To develop an anti-hIL1RAP antibody for leukemia immunotherapy, Balb/c mice were immunized with the recombinant extracellular domain (ECD) of human(h) IL1RAP (ECD, S21-E359). Plasma B cells from spleens of immunized mice were screened for IL1RAP antibody production using the Beacon® optofluidic system. Cells secreting anti-hIL1RAP antibodies were identified, and their variable heavy (V_H) and light (V_L) chain sequences were recovered by reverse transcription and determined by DNA sequencing. Twelve sets of V_H/V_L sequences were cloned into a vector containing human constant domains to create murine-human chimeric anti-IL1RAP antibodies. These antibodies were produced in ExpiCHO cells and purity (> 90%) were confirmed by size exclusion chromatography (SEC) and SDS-PAGE.

Using target monovalent affinity assay determined by surface plasmon resonance (SPR), differential scanning fluorimetry (DSF) to measure antibody thermal stability (Tm), and antibody dependent cellular cytotoxicity (ADCC) and IFN-γ release studies conducted on MV4-11 cells, we selected six candidates with the highest affinity, ADCC activity and IFN-γ release and produced their respective fragment antigen-binding regions (Fabs). Among the six Fab candidates, clone-24 showed the highest ADCC activity and IFN-γ release with a monovalent affinity of 2.2 nM and a TM of 77 °C and was therefore selected as the lead candidate. The selected variant IL1RAP-24 mAb was used to generate the TCE by Fab arm exchange (FAE) [39]. To achieve FAE, K409R and F405L mutations in the Fc CH3 domain were introduced into the anti-IL1RAP and anti-hCD3 (H26H8, a humanized anti-hCD3 mAb developed at City of Hope, manuscript in preparation) mAbs, respectively. The FAE product was verified on ion exchange chromatography (IEC). Moreover, Fc mutations abrogating CD16a binding was also generated to eliminate the Fc receptor binding [40]. The resulting TCE, BIF002 (anti-IL1RAP/CD3), is a full-length IgG1 with Fc mutations and is the lead candidate for in vitro and in vivo evaluation.

To serve as a control, point mutations were introduced into the complementarity determining regions (CDR) of each arm based on the crystal structures of IL1RAP-24 Fab and H26H8. Compared with BIF002, BiF018 contains a single point mutation in the anti-hCD3 arm and BiF026 includes two-point mutations in anti-hIL1RAP CDRs and the forementioned mutation in the anti-hCD3 arm. BiF018 and BiF026 served as controls.

Human sample collection

All primary AML (Supplementary Table 1) and healthy donor samples were obtained from the Hematopoietic Tissue Biorepository of City of Hope National Medical Center (COHNMC) under COH IRB #18067, #07047 and #06229 protocols and met the Department of Health and Human Services and Declaration of Helsinki requirements. Mononuclear cells (MNCs) were isolated using Ficoll separation. T cells were isolated from peripheral blood (PB) MNCs using EasySep™ human pan-T cells enrichment kit (StemCell Technologies, Cat #17951). For in vivo experiments, T cells were expanded with anti-CD3/CD28 Dynabeads (Gibco, Cat #11161D) at the ratio of 1:1 and 30U/L human IL-2, according to the manufacturer's instruction. Blasts were collected from newly diagnosed or relapsed AML patients. CD34+ cells were further isolated using magnetic bead selection (Miltenyi Biotec, Cat #130–046-701).

Cell culture

AML cell lines (MOLM13, MV4-11, THP-1, U937, HL60, KG1a, K562) and Jurkat cells were obtained from American Type Culture Collection (ATCC). MOLM13 and THP-1 cells were transduced with luciferase (Luci)/green fluorescent protein (GFP)—expressing lentivirus and cells with Luci/GFP + were selected for in vitro and in vivo studies. Details of the luciferase expressing human AML sample have been described previously [41]. Cell lines were cultured in RPMI1640 or IMDM supplemented with 10–20% fetal bovine serum (Gemini Bio-Products), 1% penicillin / streptomycin and 2 mM-glutamine, as described in the supplier's description. Human samples were cultured in IMDM medium containing 20% fetal bovine serum (Gemini Bio-Products), 1% penicillin/streptomycin, 2 mML-glutamine.

In vitro analyses of T cell activation and cytotoxicity

Redirected T cell cytotoxicity was assayed at 48 hour (h) using purified T cells as effector cells and AML cell lines or patient blasts or CD34+ cells as target cells, at different effector-to-target (E:T) ratios, and serial dilutions of BIF002. Target cells were stained with PKH67 Green Fluorescent Cell Linker Kit (Sigma-Aldrich, Cat #PKH67GL) one day before co-culture and distinguished from effector cells using green fluorescent protein (GFP) channel. Target cells were seeded at a density of 2×10^4 cells/200 µl. Cell death and cell apoptosis was evaluated by 7-amino actinomycin D (7-AAD) and Annexin V labeling, respectively, followed by flow cytometry analysis (FCM). Cell lysis was determined by the following formula: % Lysis = 100 − (viable cells of treatment group × 100/viable cells of untreated control group). E:T ratio of 5:1 was used for in vitro IC_{50} determination, T cell activation, and IFN-γ, TNF-α cytokine release analysis. To detect T cell activation, T cells were stained with anti-CD4, anti-CD8, anti-CD25 and anti-CD69 antibodies after 48 h of co-incubation with PHK67 labeled target cells. For cytokine release assays, IFN-γ and TNF-α in the supernatant was evaluated by ELISA Kits (BioLegend) according to the manufacturer's protocols. Intracellular IFN-γ production in T cells was also tested by FCM using the cytofix/cytoperm fixation and permeabilization solution (BD Bioscience, Cat #554722) according to the manufacturer's protocols. For T cell proliferation analysis, T cells were labeled with cell trace TM violet (CTV, Thermo Fisher, Cat #C34557) before co-culture, and after 5 days of co-culture with target cells at an E:T ratio of 2:1 or 5:1, proliferating cell percentage and division and proliferation indexes were calculated respectively using FlowJo software. Division Index is the average number of cell divisions by the original population that includes the

undivided peak. Proliferation Index is the total number of divisions divided by the number of cells that went into division.

xCELLigence eSight real time cell analysis (RTCA)

MOLM13 $^{Luci/GFP+}$ or THP-1 $^{Luci/GFP+}$ cells were seeded at a cell density of 2×10^4/200 µl per well in standard flat bottom 96 well cell culture plates and treated with healthy T cells at a prespecified E:T ratios together with serial dilutions of BIF002 (0, 0.1, 1, 10, 100 nM). Cell growth and morphology changes were monitored using a built-in automatic objective at 10x. RTCA eSight software is used for data set up, imaging acquisition schedule and data analysis. Live cell images were acquired every 30 min with 4 images/well/time in both bright-field and green fluorescence channels for 48 h. Changes of the number of GFP + target cells overtime was analyzed as Cell Index and displayed in line chart. Due to this being a real-time detection, after being placed in the machine, it takes approximately 3 h for the cells to settle and obtain clear images. Therefore, we normalized the Cell Index as subsequent GFP + cell counts at different time points to GFP + cell count at 3 h. Movies were also produced with RTCA eSight software by using composite images, at 918×758 pixels in size and presented as a speed of 2 images/s.

FCM analysis

Cells were harvested and prepared according to the manufacture's protocols. All antibodies were incubated with cells for 30 min at 4 °C unless otherwise stated. The antibodies used for FCM are described in Supplementary Table 2. All analyses were performed on Fortessa™ X-20 Cell Analyzer (BD Biosciences). Data analysis was conducted using BD FACS Diva or FlowJo software.

Cell binding

Cell binding experiments were carried out using leukemia cells and purified T cells or Jurkat cells. Jurkat cells are a line of immortalized T lymphocyte cells that express CD3 and low levels of IL1RAP. Fc receptor blocking solution (BioLegend, Cat #422301) was used to reduce the interference of target cell with Fc receptors. The generated anti-IL1RAP antibodies (or Fab) were incubated at 100 nM for 30 min at 4 °C, with the cells and after washing, incubated with anti-human Fc-PE (or anti-human Fab-Alexa 647) antibody for 15 min at 4 °C. To compare the expression levels of IL1RAP, CD33, CD123 and CLL-1 on AML blasts, Fc receptor blocking antibody and then PE-conjugated antibodies against IL1RAP, CD33, CD123 and CLL-1 (Supplementary Table 2) were incubated with AML cells and analyzed for the percentages of cells expressing the surface antigens relative to the control cells incubated with an isotype control antibody using Fortessa™ X-20 Cell Analyzer (BD Biosciences). To this end, samples with > 10% of IL1RAP-expressing cells were identified as IL1RAP + and were further divided into IL1RAP^{high} (> 50%), IL1RAP^{medium} (10–50%) and IL1RAP$^{low/neg}$ (≤ 10%).

Colony-forming cell (CFC) assays

Normal CD34+ cells obtained from health donors were co-cultured with T cells from different healthy donors at E:T ratio 5:1 and BIF002 30 nM or control BIF026 30 nM or vehicle for 24 h. After cell collection and T cell depletion using CD3 MicroBeads (Miltenyi Biotec, Cat #130–097-043), the CD34+ cells were counted and suspended in methylcellulose medium (StemCell Technologies, Cat #H4434) and placed at a density of 3,000 cells per well into 24-well plates for CFC assay. Colony-forming units (CFUs) were imaged and counted after 14 days.

In vivo studies

To assess the antileukemic efficacy of BIF002 in AML models, we generated MOLM13$^{Luci/GFP+}$ xenograft and two R/R AML PDX models. Firstly, in a dose finding experiment, MOLM13$^{Luci/GFP+}$ cells (1×10^6) were transplanted into NSG-SGM3 (NSGS) mice (6–8 weeks old, The Jackson Laboratory) (Day 0). These mice were randomly divided into four groups and treated with: vehicle alone (n = 2) or T cells alone or with 0.1 µg or 1 µg BIF002 (n = 5 mice per group). Starting on Day 3, T cells (3×10^6/mouse, E:T ratio = 3:1) from the healthy donors that have been expanded in vitro for 5–7 days were administered weekly for 5 doses. One day after T cell injection (Day 4), BIF002 was administered intravenously (IV) every 3 days (q3d) for 4 weeks. Bioimaging (BLI) was performed weekly using an in vivo imaging system. Mice were intraperitoneally injected with d-Luciferin (150 mg/kg) (Gold Biotechnology, Cat #LUCK-1G) dissolved in PBS 10 min before measuring the luminescence signal. The survival rate of each group was also recorded. Next, AML^{Luci+} blasts (AML-1, 0.5×10^6) from a relapsed/refractory (R/R) AML patient with complex karyotype were injected into 6–8 weeks old NSGS mice (Day 0). Given that a log higher IC_{50} was seen in primary cells, we treated PDX mice with T cells alone or with 1 µg, or 10 µg BIF002 (n = 5 mice per group). Starting on Day 3, T cells (1.5×10^6/mouse, E:T ratio = 3:1) were injected weekly for 4 doses. Starting on Day 4, BIF002 was administered intravenously (q3d) for 3 weeks. BLI and the survival of the mice were recorded.

Next, to confirm the antileukemic effect of BIF002, we repeated the experiment including a mutated version of BIF002 (BIF026). The AML^{Luci+} PDX mice were randomly divided into four groups and treated with 10 µg

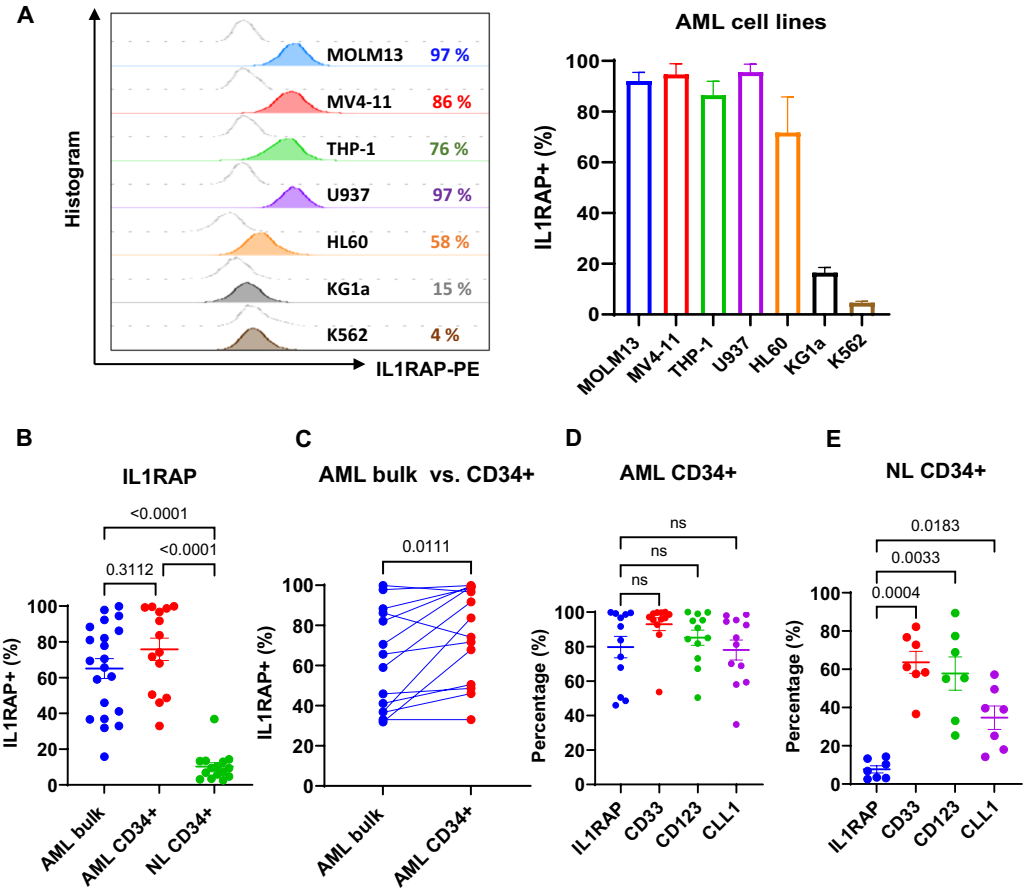

Fig. 1 IL1RAP expression on the cell surface of AML cell lines and primary AML blasts. **A** Representative histogram plots (left) and combined results (right, n = 3 independent experiments) of IL1RAP expression on AML cell lines analyzed by FCM. **B** IL1RAP expression on primary AML bulk blasts (n = 21) and AML CD34+ cells (n = 14), and normal (NL) CD34+ cells (n = 15), analyzed by FCM. **C** Paired comparison of IL1RAP expression on bulk and CD34+ blasts in individual AML patients (n = 14) by FCM. **D** Percentages of IL1RAP+, CD33+, CD123+, and CLL-1+cells in AML CD34+ blasts by FCM (n = 12). **E** Percentages of cells expressing IL1RAP, CD33, CD123, and CLL-1 relative to the control cells stained with isotype control antibody, in normal healthy donor CD34+ hematopoietic stem cells (HSCs) analyzed by FCM (n = 7). **B**, and **D**–**E** were analyzed by *one-way ANOVA* with *Tukey or Dunnett multiple comparisons tests* respectively, and **C** was analyzed by *paired Student's t-test*. NL, normal; NS, not significant

control BIF026, 10 μg BIF002, T cells + 10 μg BIF026, or T cells + 10 μg BIF002 (n = 5–7 mice per group). Similarly, starting on Day 3, T cells (1.5×10^6/mouse) were given weekly for 4 doses, and starting on day 4, 10 μg of BIF002 or BIF026 was administered intravenously for 3 weeks (q3d). BLI and the survival of the mice were recorded as described previously.

To characterize the impact of BIF002 on LSCs, a PDX model was created by engrafting blasts (AML-2, 1×10^6) from another relapsed AML patient into NSGS mice. The mice were randomly divided into 3 groups: vehicle,

(See figure on next page.)

Fig. 2 Characterization of anti-IL1RAP-24 monoclonal antibody (mAb) and production of anti-IL1RAP/CD3 bispecific T cell engager (TCE). **A** Size exclusion chromatography (SEC, left) and SDS-PAGE (right) of anti-IL1RAP-24 mAb. **B** Target affinity assay of anti-IL1RAP-24 mAb binding to IL1RAP by surface plasmon resonance (SPR). **C** Flow cytometry (FCM) analysis of binding capacity of anti-IL1RAP-24 Fab vs. isotype control antibody to $IL1RAP^{pos}$ MV4-11 and MOLM13. **D** Schematic description of anti-IL1RAP/CD3 bispecific TCEs including BIF002, BIF018 and BIF026, created by Biorender.com. **E** Ion exchange chromatography (IEC) of anti-IL1RAP/CD3 bispecific TCE (BIF002) along with parental antibodies. **F** SPR sensorgrams of TCEs, i.e., BIF002, BIF018 and BIF026, binding to CD3, IL1RAP and Fc receptor (CD16a), respectively. **G** FCM analysis of binding capacity of anti-IL1RAP or anti-CD3 commercial mAbs, anti-IL1RAP-24 mAb, and TCEs including BIF002, BIF018 and BIF026, to $IL1RAP^{high}$ AML cells and CD3+ T and Jurkat cells

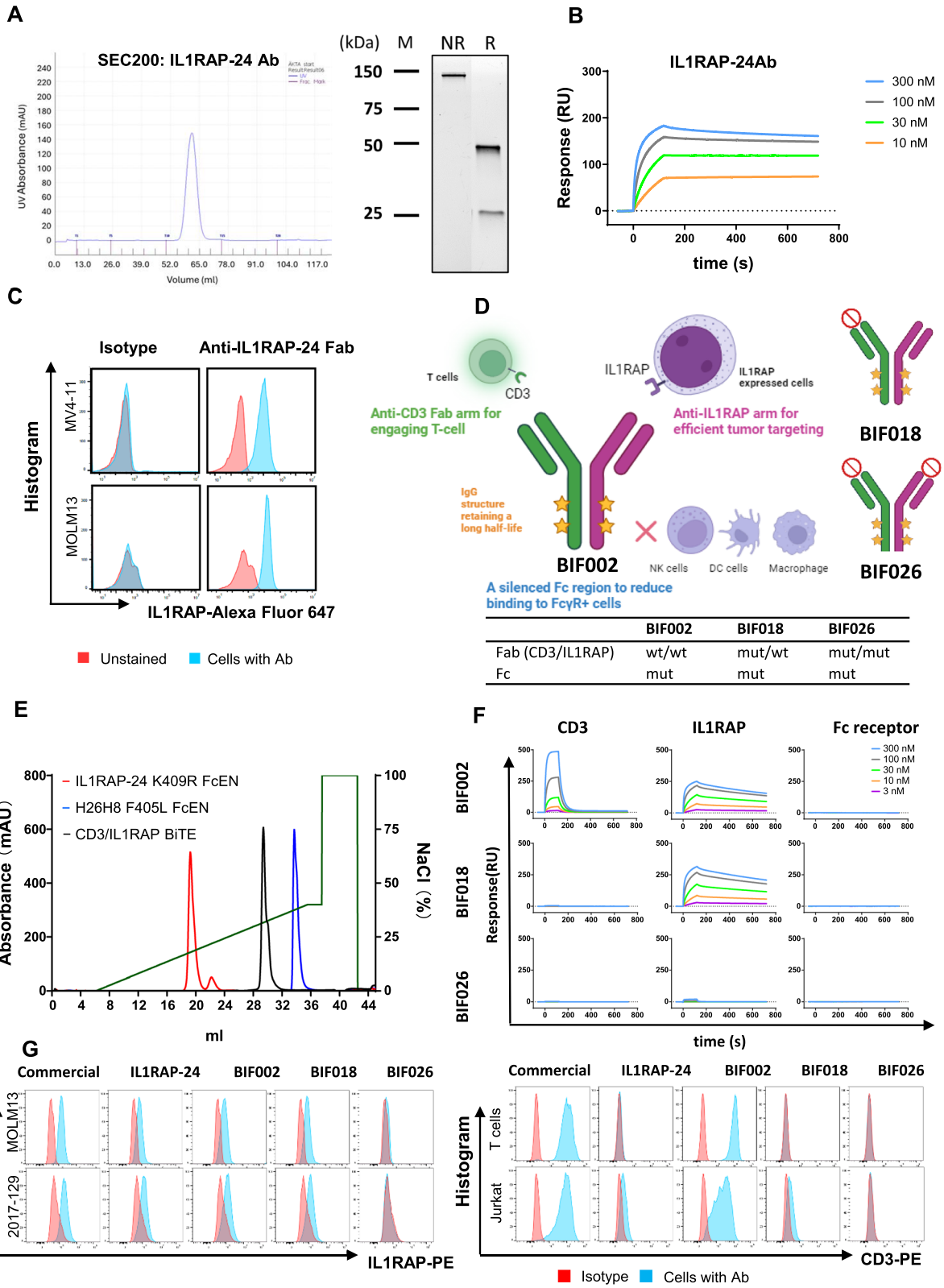

Fig. 2 (See legend on previous page.)

T cells + control BIF026, or T cells + BIF002 (n = 10 mice per group). T cells from healthy donors (3×10^6/mouse, E:T ratio = 3:1) were administered weekly for 3 doses starting on Day 10, and 10 μg BIF002 or control BIF026 started on Day 11 and continued for 3 weeks (q3d). On Day 34, BMMNCs were harvested from 3 mice/group and transplanted (1×10^6) into NSGS recipient mice (n = 7 mice per group) for evaluation of post-treatment LSCs by secondary transplantation. Human leukemic burden was analyzed by FCM. Mouse care and experiments were performed under the Institutional Animal Care and Use Committee (IACUC) approved protocol (#15005).

Statistical analysis

Statistical analyses were conducted using GraphPad Prism V.9.0.5. Group comparisons utilized *two-tailed, unpaired or paired Student t-tests* and *one-way or two-way analysis of variance (ANOVA)*. Survival comparisons were conducted using *Kaplan–Meier analysis* and the *Log-Rank test*. In vitro experiments were performed at least twice with technical duplicates or triplicates. In vivo experiments involved 5–7 mice per group. Results are presented as mean ± standard error of the mean (SEM) with significance set at $P \leq 0.05$, indicated as $^{*}P \leq 0.05$, $^{**}P < 0.01$, $^{***}P < 0.001$, or $^{****}P < 0.0001$.

Results

High IL1RAP expression on AML cell lines and patients' blasts

We assessed IL1RAP expression levels on representative AML cell lines (MOLM13, MV4-11, THP-1, U937, HL60, KG1a), primary AML bulk blasts and CD34+ blasts, and normal CD34+ BM cells by flow cytometry (FCM). AML cell lines showed high expression of IL1RAP ($IL1RAP^{high}$; i.e., > 50% IL1RAP + cells), except for KG1a ($IL1RAP^{medium}$; 16%) and K562 ($IL1RAP^{low/neg}$; 5%) (Fig. 1A). Primary AML bulk blasts ($IL1RAP^{high}$; 65% ± 5%; n = 21) and $CD34^+$ blasts ($IL1RAP^{high}$;76 ± 6%, n = 14) also expressed significantly higher levels of IL1RAP than normal $CD34^+$ BM cells ($IL1RAP^{low/neg}$;10 ± 2%; n = 15; $p < 0.0001$; Fig. 1B). Notably, in the same patient, the frequency of IL1RAP + cells were higher in LSC-enriched CD34+ population than in bulk blasts (n = 14, $p = 0.011$; Fig. 1C). Compared with other AML surface antigens that are currently being pursued as therapeutic targets in the clinic [i.e., CD33 (93 ± 4%), CD123 (85 ± 4%) or CLL-1(78 ± 6%)], IL1RAP expression (80 ± 6%) was similar in $CD34^+$ blasts (Fig. 1D), but significantly lower in normal $CD34^+$ cells from healthy donors (IL1RAP+: 8 ± 2%; CD33+: 64 ± 6%; CD123+: 58 ± 9%, CLL-1+: 35 ± 6%; Fig. 1E).

Development and characterization of the novel anti-IL1RAP/CD3 T cell engager (TCE) BIF002

To target IL1RAP + AML blasts, next, we developed an anti-hIL1RAP antibody. Briefly, Balb/c mice were immunized with the recombinant ECD of hIL1RAP (S21-E359). Plasma B cells from the spleens of the immunized mice were screened for IL1RAP antibody production, cells secreting anti-hIL1RAP antibodies identified and their variable heavy (V_H) and light (V_L) chain sequences determined. Out of 108 positive hits from single B cells, we successfully recovered 34 sets of V_H/V_L sequences, from which we selected twelve mAb candidates based on the sequence diversity of the CDRs. The twelve V_H/

(See figure on next page.)

Fig. 3 Dose-and effector-to-target (E:T) ratio-dependent activity of BIF002. **A** Cell lysis of MOLM13 and THP-1 at different E:T ratios and various concentrations of BIF002 at 48 h (normalized to no Ab ctrl at same E:T ratio; n = 3). The experiment was repeated with another T cell donor, and similar results were obtained. **B** Real-time counts of GFP + target AML cells from co-cultures with BIF002 (0.1—100 nM) and T cells (E:T ratio 5:1) (upper), and representative real time fluorescence plots of GFP + THP-1 lysis by BIF002 at E:T ratio 5:1 (lower), recorded by Agilent xCELLigence (technical duplicate). The experiment was repeated with another T cell donor, and similar results were obtained. Cell index was normalized to GFP + cell counts at 3 h of the same well. **C** Viability changes (left; n = 3) and combined IC_{50} results (right; n = 3 independent T cell donors) of AML cell lines treated with BIF002 and T cells at E:T ratio 5:1 at 48 h. The experiment was repeated with two other T cell donors, and similar results were obtained. **D**–**E** Viability changes of primary AML bulk blasts (**D**; n = 3) and AML CD34+ blasts (**E**; n = 3) treated with BIF002 and T cells at E:T ratio 5:1 at 48 h. **F** Cell lysis of AML CD34+ blasts (n = 3) treated with healthy donor T cells and BIF002, or BIF016, or BIF026 at E:T ratio 5:1 at 48 h. **G** Cell lysis of AML cell lines treated with healthy donor PBMC and BIF002, or BIF016, or BIF026 at E:T ratio 5:1 at 48 h (n = 3). The experiment was repeated with another T cell donor, and similar results were obtained. **H** Combined results (left; n = 5 samples) and representative plots (right) of apoptotic cells in primary AML blasts treated with healthy donor T cells and BIF002 or BIF026 control at E:T ratio of 5:1 at 48 h. **I** Viability of normal (NL) CD34+ bone marrow cells treated with healthy donor T cells and BIF002 at E:T ratio 5:1 at 48 h (n = 3). **J** Normal CD34+ cells were treated with T cells and BIF002 or BIF026 (30 nM) or vehicle at E:T ratio 5:1 for 24 h and then cultured for colony-forming cell (CFC) assay. Representative colonies (left) and quantification (right; n = 3) of CFCs on Day 14 normalized to vehicle were shown. The experiment was repeated with another T cell donor, and similar results were obtained. Except for a various E:T ratio in A and the use of PBMC as effector cells in G, the effector cells for the others are healthy donor T cells with an E:T ratio of 5:1. Cell death was evaluated by 7-amino actinomycin D (7-AAD+) labeling. Apoptotic cells were evaluated by 7-amino actinomycin D (7-AAD+) or Annexin V (+) labeling. AML lysis was determined by the following formula: % Lysis = 100 – (viable cells of treatment group × 100/viable cells of untreated control group)

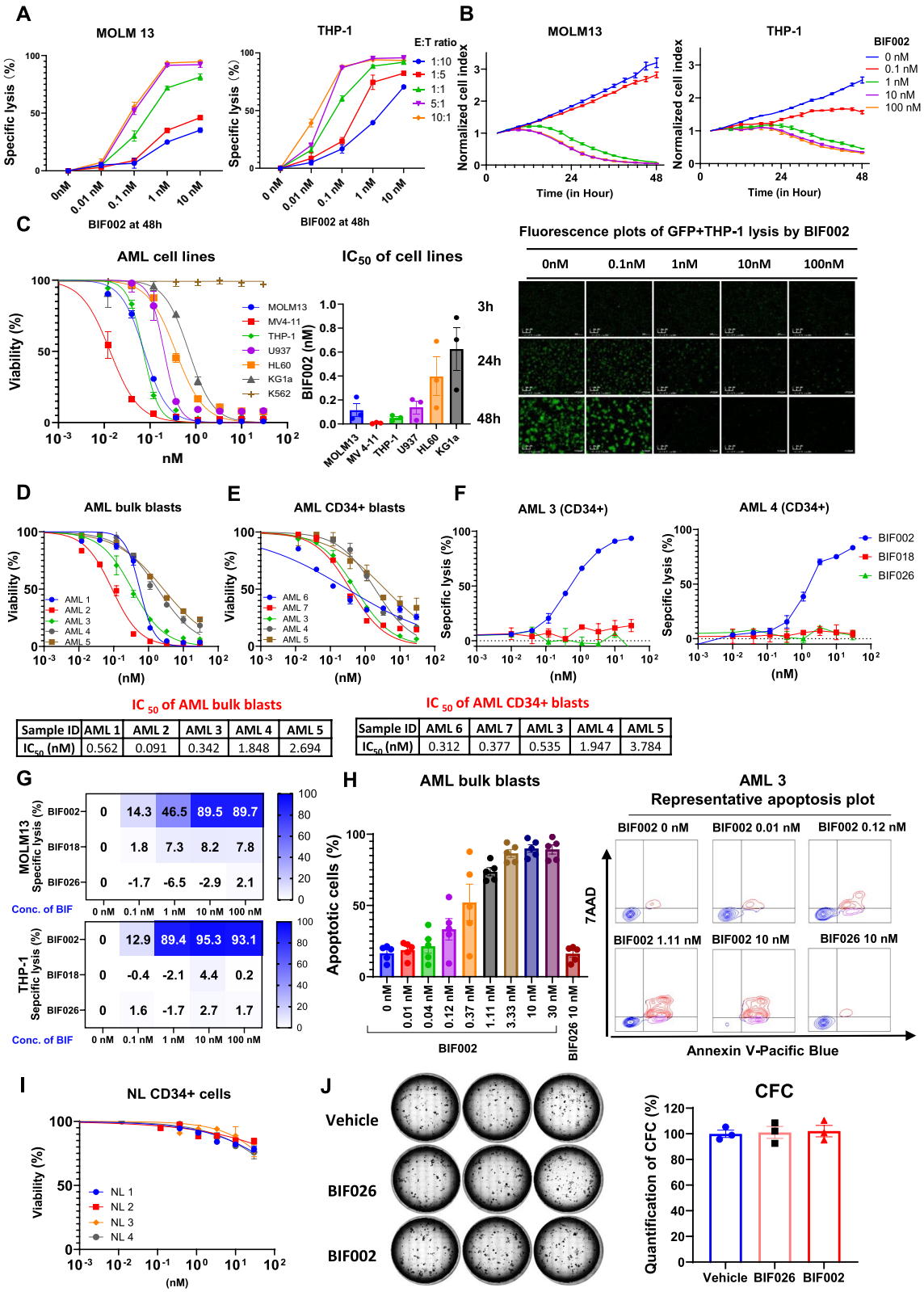

Sample ID	AML 1	AML 2	AML 3	AML 4	AML 5
IC_{50} (nM)	0.562	0.091	0.342	1.848	2.694

Sample ID	AML 6	AML 7	AML 3	AML 4	AML 5
IC_{50} (nM)	0.312	0.377	0.535	1.947	3.784

Fig. 3 (See legend on previous page.)

V_L sequences were then cloned into a vector containing human constant domains to create murine-human chimeric anti-IL1RAP antibodies. Using size exclusion chromatography (SEC; Supplementary Fig. 1A), a target affinity assay determined by SPR (Supplementary Fig. 1B), differential scanning fluorimetry (DSF) to measure antibody thermal stability (Tm; not shown), and ADCC and IFN-γ release studies conducted on MV4-11 cells (not shown), we selected six candidates with the highest affinity, ADCC activity and IFN-γ release and produced their respective Fabs (Supplementary Fig. 2A–C). Among the six candidates, clone #24 (IL1RAP-24) showed the highest activity with a monovalent affinity of 2.2 nM and a T_M of 77 °C (Supplementary Fig. 2A–C) and was therefore selected as the lead candidate (Fig. 2A–C). Crystallographic data and refinement for IL1RAP-24 Fab are shown in Supplementary Table 3. Of note, IL1RAP-24 Ab showed no cross-reactivity with normal human tissues, i.e., liver, lung, and brain, by immunohistochemical (IHC) staining (Supplementary Fig. 3).

Next, we used the IL1RAP-24 clone and FAE to produce anti-IL1RAPxCD3 TCEs (Fig. 2D; see methods for details). Using IEC to distinguish the anti-IL1RAPxCD3 TCEs from the parental antibodies (Fig. 2E), SPR to measure the binding of the TCEs to the cognate targets (i.e., CD3 and IL1RAP; Fig. 2F), and FCM analysis to measure the binding of the TCEs to IL1RAP+ AML cells and CD3+ T cells (Fig. 2G), we selected the anti-IL1RAP/CD3 TCE BIF002, a full-length IgG1 with Fc mutations, as lead candidate and evaluated it's in vitro and in vivo activity.

To obtain mutated controls and address binding specificity, we introduced point mutations into the CDR of each arm based on the crystal structures of IL1RAP-24 Fab (Fig. 2D; Supplementary Fig. 4A–E) and H26H8 (Fig. 2D). BiF018 consisted of anti-hIL1RAP partnered with a mutated anti-hCD3 arm and incorporates a mutant Fc abrogating binding to Fc binding receptors. BiF026 included two point-mutations in the anti-hIL-1RAP arm to abrogate IL1RAP binding (i.e., I30S and Q99E; Supplementary Fig. 4D) and was paired with the aforementioned mutated anti-hCD3 arm and Fc. BiF018 and BiF026 served as control constructs (Fig. 2D). As expected, while BIF018 bound to IL1RAP, and not to CD3, BIF026 did not bind to either target (Fig. 2F-G).

Next, we tested if BIF002 inhibited IL-1 signaling in target cells. First, we compared the response of HEK-Blue™ IL-1β cells (InvivoGen) to IL-1α/IL-1β in the presence of BIF002 or the commercial anti-IL1RAP Ab nidanilimab (ThermoFisher, #MA5-42,255). Dose-dependent inhibition of IL-1 signaling in HEK-Blue™ IL-1β cells was observed in the presence of nidanilimab when cells are treated with IL-1α or IL-1β, but not at the concentrations of BIF002 needed to eliminate the target (Supplemental Fig. 5A, B). We also treated MOLM13 cells with our IL1RAP-24 Ab (20 μg/ml; 133 nM) or BIF002 (5 μg/ml; 33 nM) or the commercial anti-IL1RAP Ab nidanilimab. Western blot analysis showed a reduction of phospho-IRAK1 and phospho-p38 levels in nidanilimab-treated cells, but not in IL1RAP-24 Ab-treated or BIF002-treated cells (Supplemental Fig. 5C, D). Taken altogether, these findings support that IL1RAP-24 Ab and BIF002 do not have an IL1RAP-signal blocking activity.

BiF002 activity on AML cells

To test the antileukemic activity of BIF002, we co-cultured healthy donor T cells with AML cell lines MOLM13 or THP-1 cells at different E:T ratios (range: 1:10 to 10:1) and serial concentrations of BIF002 (range: 0.01–10 nM) for 48 h. We observed a dose- and E:T ratio- dependent cell lysis (Fig. 3A). At 48 h, a near 100% target AML cell lysis was observed at E:T ratio ≥ 5:1 and BIF002 ≥ 1 nM.

The BIF002-dependent AML cell lysis was documented in real time using MOLM13$^{Luci/GFP}$ and THP-1$^{Luci/GFP}$

(See figure on next page.)

Fig. 4 BIF002 induces IL1RAP dose-dependent T cell activation, cytokine release and T cell proliferation. **A** T cell activation, assessed by CD69 and CD25 expression levels analyzed by FCM, after co-culture with AML cell lines (top; vehicle-treated MOLM13 as control; n = 3 independent T cell donors) or primary AML blasts with different IL1RAP expression levels (bottom; vehicle-treated AML-2 as control; n = 3) at E:T ratio 5:1 for 48 h assessed by CD69 and CD25 expression levels. **B** BIF002 dose-dependent T cell activation after co-culture with AML cell lines (top; n = 3 independent T cell donors) or primary AML blasts with different IL1RAP expression levels (bottom; n = 3) at E:T ratio 5:1 for 48 h, assessed by CD69 and CD25 expression levels analyzed by FCM. IFN- γ (**C**) and TNF-α (**D**) release test in T cells co-cultured with AML cell lines and blasts and treated with BIF002 for 48 h, analyzed by ELISA (technical duplicate). The experiment was repeated with another donor, and similar results were obtained. **E** T cells were stained with CellTrace violet prior to co-culture with AML cell lines and BIF002 1 nM at E:T ratio 2:1 or 5:1 for 5 days. Representative plots of violet peaks representing successive generations of T cells (upper), and proliferation indexes (lower) of T cells after 5 days of co-culture (technical duplicate). Each successively dimer peak represents one cell division. Division Index is the average number of cell divisions by the original population that includes the undivided peak. Proliferation Index is the total number of divisions divided by the number of cells that went into division. All calculated by Flowjo. The data were analyzed by *one-way ANOVA*. AML cell lines were compared to KG1a which causes low T cell proliferation in the co-culture system. Additionally, no T cell proliferation was observed when co-cultured with K562, indicating a clear difference compared to other AML cell lines. **F** T cells were stained with CellTrace violet prior to co-culture with AML blasts and BIF002 at E:T ratio 2:1 for 5 days. Representative plots of violet peaks representing successive generations of T cells. Significance values: $^{**}p < 0.01$; $^{***}p < 0.001$; $^{****}p < 0.0001$

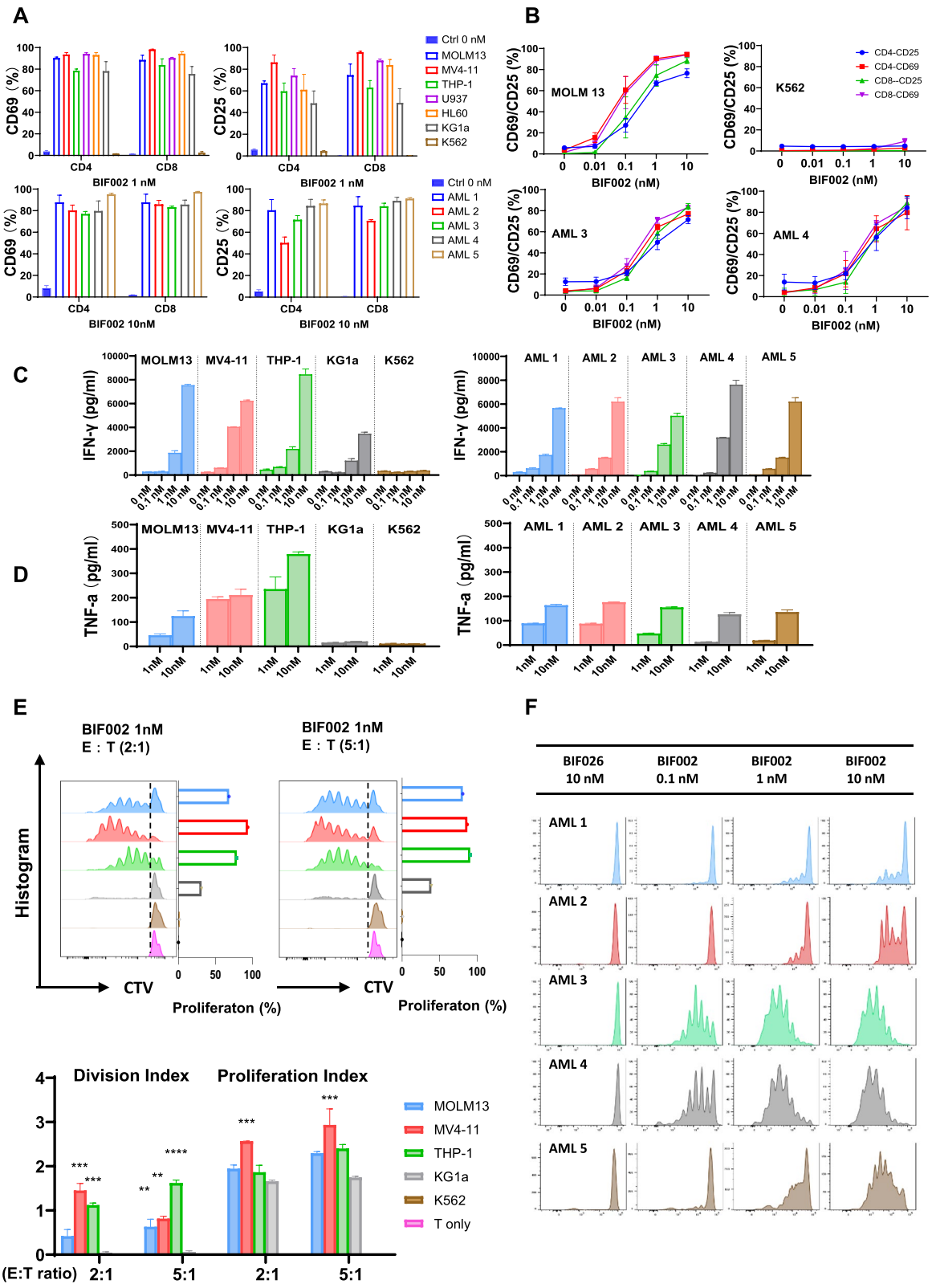

Fig. 4 (See legend on previous page.)

cells treated with BIF002 (range 0.1–100 nM) and T cells, and imaging with xCELLigence RTCA eSight platform that recorded the dynamic changes of the GFP+ AML signals over time. At E:T ratio of 5:1, in the absence of the BIF002, T cells displayed no AML cytolytic activity, while starting at 0.1 nM BIF002 concentration, the T cell cytolytic activity increased in a dose- and time-dependent manner (Fig. 3B). Of note, at E:T ratio 5:1, 10 nM BIF002 produced a significant T cell proliferation and IL1RAP+MOLM13 and THP-1 lysis (Supplementary Video 1. MOLM13 and Video 2.THP-1).

After 48 h exposure, starting with resting T cells and an E:T ratio of 5:1, the BIF002 IC_{50} was found to be within a subnanomolar range (Fig. 3C), and seems to correlate inversely with IL1RAP expression levels (Fig. 1A). In fact, while IL1RAP+ AML cells were killed in the presence of BIF002, IL1RAP$^{low/neg}$ K562 cells remained viable. The median IC_{50s} for IL1RAP^{pos} AML bulk and CD34+ blasts were also in subnanomolar ranges [0.56 nM (range 0.09–2.69 nM, n = 5, Fig. 3D) and 0.53 nM (range: 0.31–3.78 nM, n = 5, Fig. 3E), respectively]. Comparing the cytotoxic effects of BIF002 on bulk and CD34+ blasts from primary AML3, AML4, and AML5 samples, we observed similar BIF002 cytotoxic effects on both AML bulk and CD34+ blasts (Supplementary Fig. 6).

Next, we tested the specificity of BIF002 using BIF018 and BIF026 as controls. After 48 h co-culture of the AML CD34+ blasts with *FLT3-ITD* mutations (AML-3 and AML-4), at E:T ratio of 5:1, while BIF002 exposure increased AML cell lysis, neither BIF018 nor BIF026 killed the cells (Fig. 3F). Similar results were observed using PBMC (E: T at 5:1) as the source of T effector cells (Fig. 3G). We also observed an increase in apoptosis of IL1RAP^{pos} primary AML blasts (n = 5) after treatment with BIF002, and not with BIF026 (Fig. 3H). Of note, no cell killing was observed when either AML or T cells alone were treated with BIF002 or BIF026 (Supplementary Fig. 7A-C). Importantly, no significant changes in the viability of normal CD34+ BM cells (n = 4) were observed when they were co-cultured with T cells and BIF002 (Fig. 3I). Furthermore, no difference on CFCs was observed in normal CD34+ BM cells co-cultured with BIF002 and T cells compared with those co-cultured with T cells alone or with BIF026 and T cells (Fig. 3J), supporting that BIF002 cytotoxicity spared normal HSCs.

BIF002 induces dose-dependent T cell activation, cytokine release and proliferation

To test BIF002-induced T cells activation, AML cell lines or primary blasts were incubated with BIF002 (range 0.01–10 nM) and T cells at E:T ratio 5:1 for 48 h. T cells co-cultured with IL1RAP^{pos} AML cells and BIF002 had a dose-dependent increase in the levels of activation marker CD25 and CD69 on both CD4+ and CD8+ subpopulations (Fig. 4A, B), and a dose-dependent increase in IFN-γ (BIF002 0.1 to 10 nM) and TNF-α (BIF002 1 to 10 nM) production as measured by ELISA (Fig. 4C, D), compared to untreated control cells. We confirmed these results with intracellular FCM, showing that BIF002 (0.1–10 nM) induced a dose-dependent IFN-γ production in T cells when incubated with AML cells for 48 h (Supplementary Fig. 8).

To assess BIF002-induced T cell proliferation, we labeled T cells with cell trace ™ violet (CTV, Invitrogen) and incubated them with AML cell lines or primary blasts at E:T ratio of 2:1 or 5:1 in the presence of BIF002. On day 5, T cells' proliferation was significantly increased, as indicated by multipeaked CTV signal and increased division and proliferation indexes (Fig. 4E, F). This effect was observed for both CD4+ and CD8+ T cell subpopulations (Supplementary Fig. 9A, B). T cell activation was not observed in co-cultures with IL1RAP$^{low/neg}$ cells (i.e., K562) in the presence of BIF002 or with IL1RAP^{pos} AML cells (i.e., MOLM13, MV4-11, THP-1, U937, HL60, KG1a and blast) in the absence of BIF002 (Fig. 4 A-C, E and F), suggesting that specific binding of BIF002 to both IL1RAP and CD3 antigens respectively on AML and T cells, was required for T cell activation and proliferation.

In vivo *activity of BIF002*

To investigate the in vivo activity of BIF002, we first generated MOLM13^{Luci} xenograft by transplanting MOLM13^{Luci} cells into NSGS mice and divided the mice randomly into 4 groups which were treated with 0.1 or 1 μg BIF002 q3d and in vitro Dynabead expanded healthy

(See figure on next page.)

Fig. 5 In vivo efficacy and dose finding of BIF002 in AML mice models. **A** Schematic experimental design. Luciferase-expressing MOLM13 were transplanted into NSGS mice that were treated with: vehicle alone (n = 2) or T cells alone or with 0.1 μg or 1 μg BIF002 (n = 5 mice per group). **B** Tumor burden assessed using bioluminescent imaging of MOLM13-engrafted mice. **C** Quantitation of total bioluminescent signal (Total Emission) in each group at indicated times post-injection for MOLM13 model. **D** *Log-rank (Mantel-Cox) test* of cumulative survival rates for MOLM13-engrafted mice. **E** Schematic experimental design. Luciferase-expressing AML patient cells were transplanted into NSGS mice (PDX model). These mice were treated with: T cells alone or with 1 μg or 10 μg BIF002 (n = 5 mice per group). **F** Tumor burden assessed using bioluminescent imaging of PDX mice. **G** Quantitation of total bioluminescent signal of PDX mice. **H** *Log-rank (Mantel-Cox)* test of cumulative survival rates for PDX model. C and H were analyzed by *two-way ANOVA* with *Tukey multiple comparisons tests*. Significance values: *$p < 0.05$; **$p < 0.01$; ***$p < 0.001$; ****$p < 0.0001$

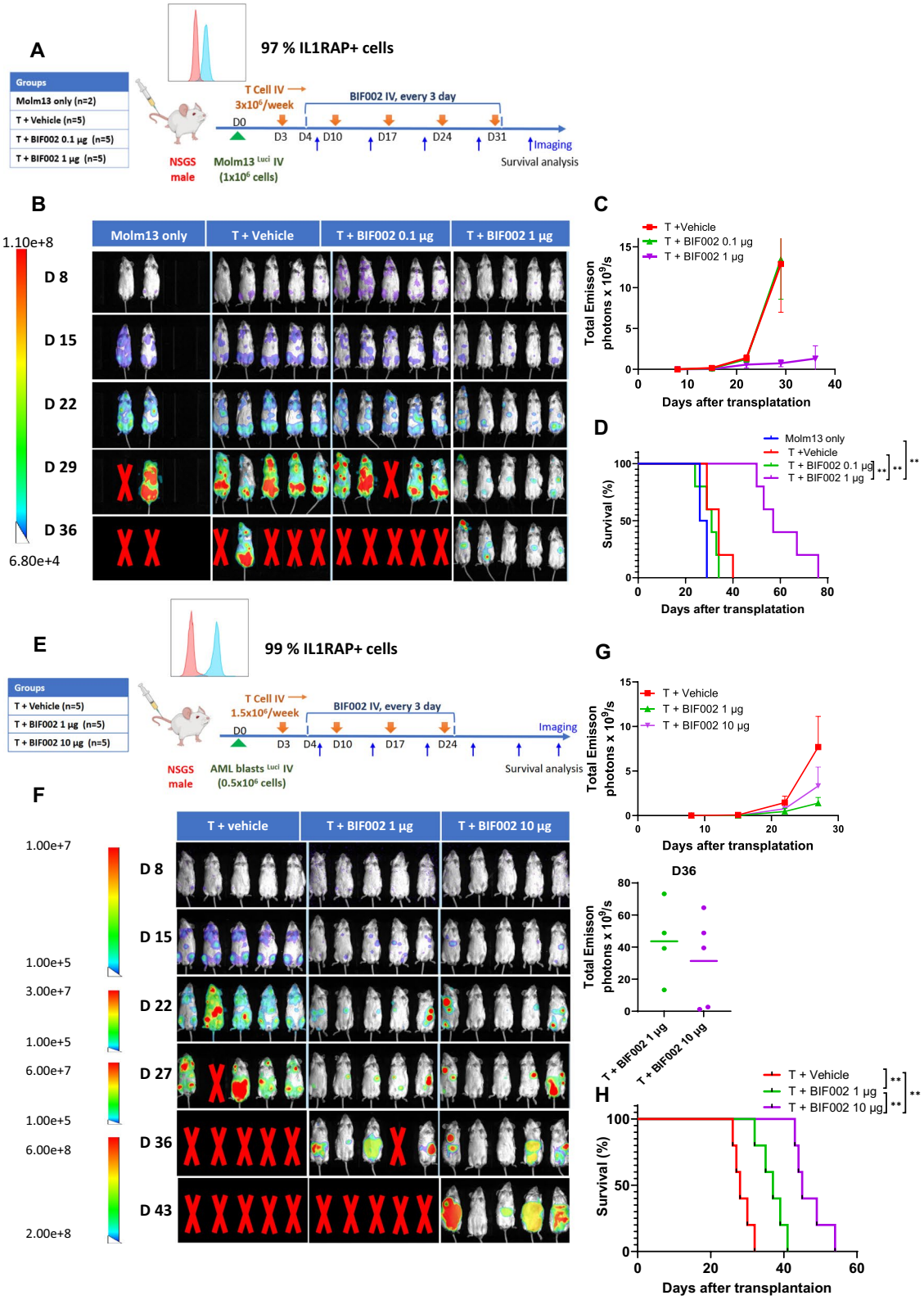

Fig. 5 (See legend on previous page.)

donor T cells, or T cells alone (n = 5) or vehicle (n = 2) (Fig. 5A). Mice treated with T cells + 1 μg of BIF002 had significantly lower tumor burden compared to the mice treated with T cells + 0.1 μg of BIF002 ($p = 0.0014$) or T cells alone ($p = 0.0186$) as measured by bioluminescence imaging (Fig. 5B, C) and survived significantly longer (median survival: 57 days) than the mice treated with T cells + 0.1 μg of BIF002 (31 days, $p = 0.0018$), T cells alone (34 days, $p = 0.0019$) or vehicle (27.5 days, $p = 0.0082$) (Fig. 5D).

Based on these dose-finding results and on the higher IC_{50} we observed in primary blasts vs Molm13 cells, we then generated a PDX model by transplanting luciferase-expressing blasts (IL1RAP + cells 99%) from a complex karyotype R/R AML patient into NSGS mice and treated these mice with either 1 or 10 μg of BIF002 q3d and healthy donor T cells, or vehicle plus T cells (n = 5; Fig. 5E). Starting from Day 15, mice treated with T cells plus 1 μg ($p = 0.0017$) or 10 μg ($p = 0.0008$) of BIF002 exhibited a reduction in leukemia burden compared to the T cells + vehicle-treated mice measured by luminescence signals (Fig. 5F-G). Treatment with 10 μg BIF002+T cells resulted in a significantly longer survival (median: 45 days) than treatment with 1 μg BIF002+T cells (37 days, $p = 0.0018$) or vehicle + T cells (28 days, $p = 0.0018$) (Fig. 5H).

To confirm these results, we repeated this experiment by treating the luciferase-expressing PDX mice with 10 μg BIF002 or the mutated control antibody BIF026 to confirm the specificity of BIF002, q3d for 3 weeks (Fig. 6A). Mice treated with T cells + BIF002 had 20 to 70-fold reduction in disease burden measured by luminescence signals and fewer circulating blasts and eventually survived longer than the mice treated with control antibody BIF026, BIF002 alone, or T cells + BIF026 (median survival: 46 vs 26, 25 or 30 days, respectively, $p = 0.0003$ for each group compared to T cells + BIF002) (Fig. 6B–E). All the mice eventually died of leukemia after the treatment was stopped.

To explore if BIF002 targeted LSCs, we then generated a PDX model by transplanting primary blasts from a relapsed, complex karyotype AML patient with 93% IL1RAP + cells into NSGS mice (Fig. 7A) and treated these mice with T cells plus 10 μg BIF002 or control BIF026 or vehicle, starting on day 10 after transplant, for 3 weeks. On day 28, we observed a significant reduction of circulating blasts in the mice receiving T cells + BIF002 (0%) compared with those receiving T cells + BIF026 (35.1 ± 7.4%, $p = 0.0006$) or vehicle (34.7 ± 6.9%, $p = 0.0007$) (Fig. 7B, C). After monitoring for 70 days post-transplant, all the mice treated with T cells + BIF002 were alive, with no detectable PB or BM blasts, while all T cells + BIF026 (median survival: 38 days, $p = 0.0001$) or vehicle (38 days, $p = 0.0002$) -treated mice had already died of leukemia (Fig. 7B, D).

For the secondary (2nd) transplant experiment, we then randomly selected 3 female mice from each group on day 34 post-transplant, harvested BM and transplanted 10^6 MNCs into 2nd NSGS recipients (n = 7 per group). At the time of the BM harvest, the donors treated with vehicle (spleen weight 0.447 g, $p = 0.0033$) or T + BIF026 (0.565 g, $p = 0.0008$) had significantly larger spleens than those treated with T + BIF002 (0.072 g) (Fig. 7E). Near 100% PB and BM blasts and 70% splenic blasts were detected in the mice treated with T + BIF026 or vehicle, while leukemia clearance (1.3%, 0.2%, 0.4% PB, BM and splenic blasts, respectively) was observed in the T cells + BIF002 treated group (Fig. 7F-G). Of note, treatment with T cells + BIF002 eliminated LSCs as supported by lack of disease on Day 21 after transplantation, in the 2nd recipients of BMMNCs from T + BIF002-treated donors compared with the recipients of BMMNCs from vehicle- (34.3 ± 5.6%, $p < 0.0001$) or T + BIF026- (32.5 ± 5.2%, $p = 0.0002$) treated donors (Fig. 7H). Of note, all the recipients of T + BIF002-treated donor BM survived over 200 days, and the recipients of BM from vehicle (median survival 26 days; $p = 0.0004$) or T cells + BIF026 (26 days; $p = 0.0002$) -treated donor BM died within 30 days (Fig. 7I). At the end of the observation, none of the mice transplanted with T cell + BIF002-treated donor BM showed detectable blasts in the PB and BM, suggesting LSCs were eradicated.

Discussion

Recently, IL1RAP has emerged as a promising target for cancer immunotherapy as this antigen is significantly upregulated on the surface of leukemia and cancer cells compared to the counterpart normal cells [29, 42, 43]. High IL1RAP expression likely contributes to malignant cell growth through the amplification of inflammatory and antioxidant driving mechanisms and is associated with significantly worse clinical outcomes

(See figure on next page.)

Fig. 6 In vivo efficacy of BIF002 in the luciferase-expressing AML PDX Model. **A** Schematic experimental design. Luciferase-expressing AML patient cells were transplanted into NSGS mice that were then treated with: 10 μg control Ab BIF026, 10 μg BIF002, T cells + 10 μg BIF026, or T cells + 10 μg BIF002 (n = 5–7 mice per group). **B** Tumor burden assessed using bioluminescent imaging. **C** Quantitation of total bioluminescent signal (Total Emission) in each group at indicated times post-injection. **D** *Log-rank (Mantel-Cox) test* of cumulative survival rates. **E** Representative Wright-Giemsa stain of peripheral blood by microscope (n = 2, 1000X magnification). Significance values: *$p < 0.05$; **$p < 0.01$; ***$p < 0.001$; ****$p < 0.0001$

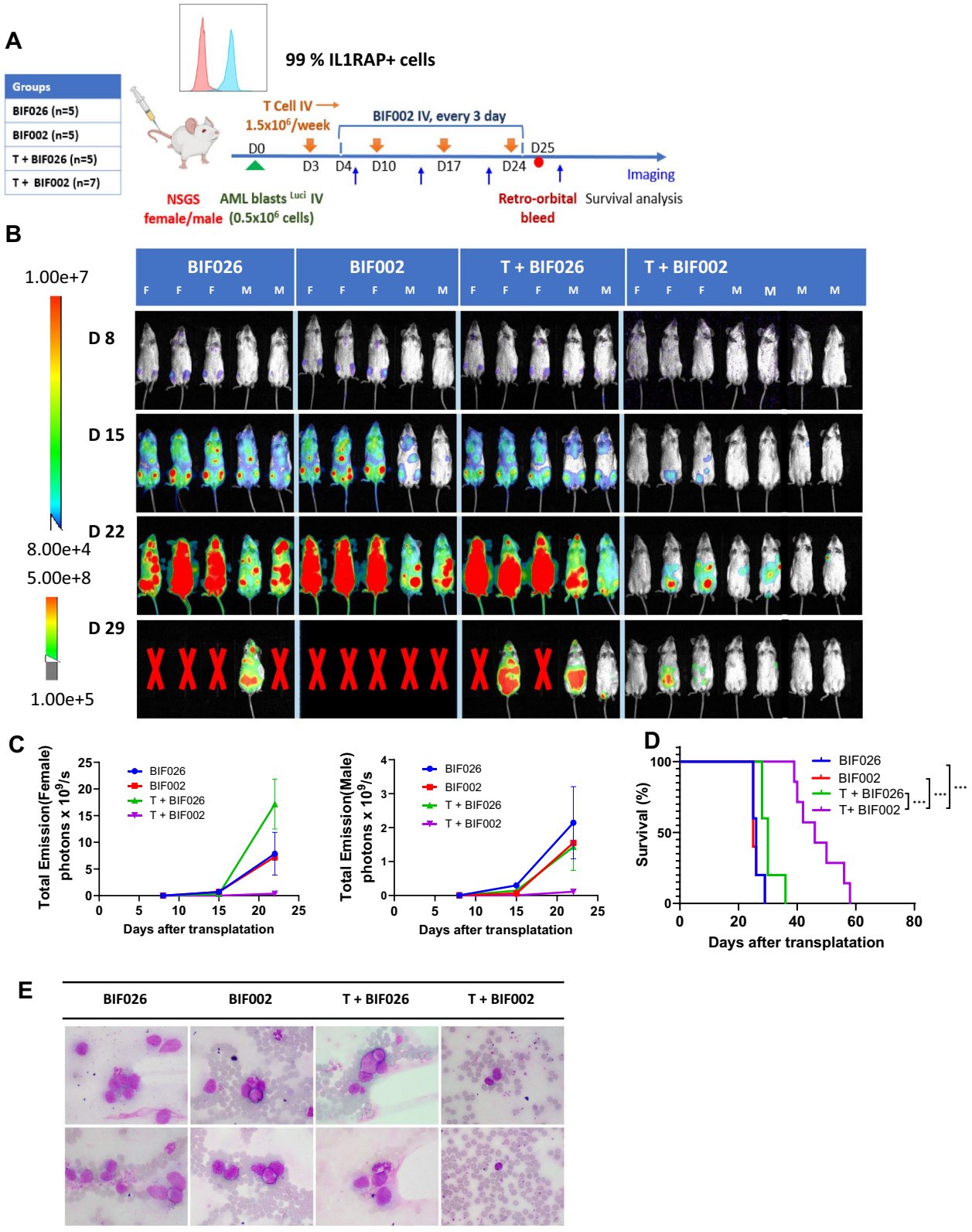

Fig. 6 (See legend on previous page.)

[28]. A previous report by Askmyr, et al., suggested that approximately 80% of AML patients have medium to high IL1RAP expression levels [32]. Barreyro et al. reported higher IL1RAP levels in MDS/secondary AML carrying monosomy 7 [30]. Herein, we showed that IL1RAP is highly expressed on LSC-enriched AML CD34+ blasts from both de novo and relapsed patients. Thus, it is likely that IL1RAP-directed therapeutic approaches could benefit a relatively large proportion of AML patients. Of note, compared to other AML surface antigens that are already being targeted in the clinic (i.e., CD33, CD123 and CLL-1), IL1RAP showed lower expression on HSPCs, supporting its specificity for AML blasts.

To date, while IL1RAP-targeting immunotherapeutics are being developed in solid tumors [37, 38] including nadunolimab, a monoclonal IL1RAP antibody [44], as a single agent (NCT03267316) or in combination with other immunotherapeutics (NCT04452214) or with chemotherapy (NCT04990037; NCT05116891; NCT05181462) and IL1RAP targeting chimeric antigen receptor T cells (CAR-T) are also being tested in early clinical trials of CML (NCT02842320) and AML (NCT04169022), to our knowledge IL1-RAP TCEs have not been reported.

Herein, we described the design, selection, and characterization of a novel CD3-IL1RAP TCE. We show that BIF002 efficiently binds to IL1RAP^{pos} AML cells and CD3^{pos} T cells, activates T cells, and directs the engaged T cells to lyse IL1RAP^{pos} AML cells. Importantly, we showed not only a strong antileukemic activity of BIF002 against bulk blasts in PDXs, but also the ability of TCE to eradicate LSCs. In fact, in secondary transplantation experiments, all recipients of BMMNCs from primary donors treated with T cells + BIF002 were alive after more than 200 days post-transplant, without any further treatment. In contrast, all the recipients of BMMNCs from primary donors treated with T cells + control mAb BIF026 or vehicle succumbed to disease with a median OS of only 26 days. Of note, we observed no in vivo toxicity in our preliminary non-GLP study. In fact, mice treated with BF002 alone or in combination with T cells had no weight loss, behavioral changes or evidence of GVHD. Furthermore, in preliminary in vitro experiments, we observed no inhibition of normal hematopoietic activity.

In summary, our data support a strong antileukemic activity of BIF002, that selectively redirects T cells to kill both AML bulk blasts and LSCs, with no apparent hematologic or non-hematologic toxicities. While these results are preliminary, IND-enabling studies including pharmacokinetics and pharmacodynamics (PK/PD) and additional toxicology studies are underway to rapidly translate this promising TCE from the bench to the bedside.

(See figure on next page.)

Fig. 7 In vivo efficacy of BIF002 in the AML PDX Model with second transplantation. **A** Schematic experimental design. Blasts from a relapsed AML patient were transplanted into NSGS mice that were then treated with: vehicle, T cells + 10 µg control BIF026, or T cells + 10 µg BIF002 (n = 10 mice per group). On Day 34, BMMNCs were harvested from 3 mice/group and transplanted into NSGS recipient mice (n = 7/group) without further treatment. **B** Blasts and human T cell populations at Day 28 (upper) and at Day 70 (lower) by flow cytometry (FCM). **C** Representative Flow plots of blasts and T cells at Day 28 (n = 2). **D** *Log-rank (Mantel-Cox) test* of cumulative survival rates on first transplantation (n = 7). **E** Spleen size and weight of different groups. **F** Blasts and human T cell populations in bone marrow, peripheral blood, and spleen at the time for the second transplantation by FCM (n = 3). **G** Wright-Giemsa stain of peripheral blood by microscope (n = 3, 1000X magnification). **H** Blasts and human T cell populations at Day 21 in second transplantation mice peripheral blood by FCM. **I** *Log-rank (Mantel-Cox)* test of cumulative survival rates on the second transplantation (n = 7). B (left), E and H were analyzed by *one-way ANOVA* with *Tukey multiple comparisons tests*, F were analyzed by *two-way ANOVA* with *Tukey multiple comparisons tests*, and B(right) were analyzed by *unpaired Student's t test*. Significance values: *$p < 0.05$; **$p < 0.01$; ***$p < 0.001$; ****$p < 0.0001$

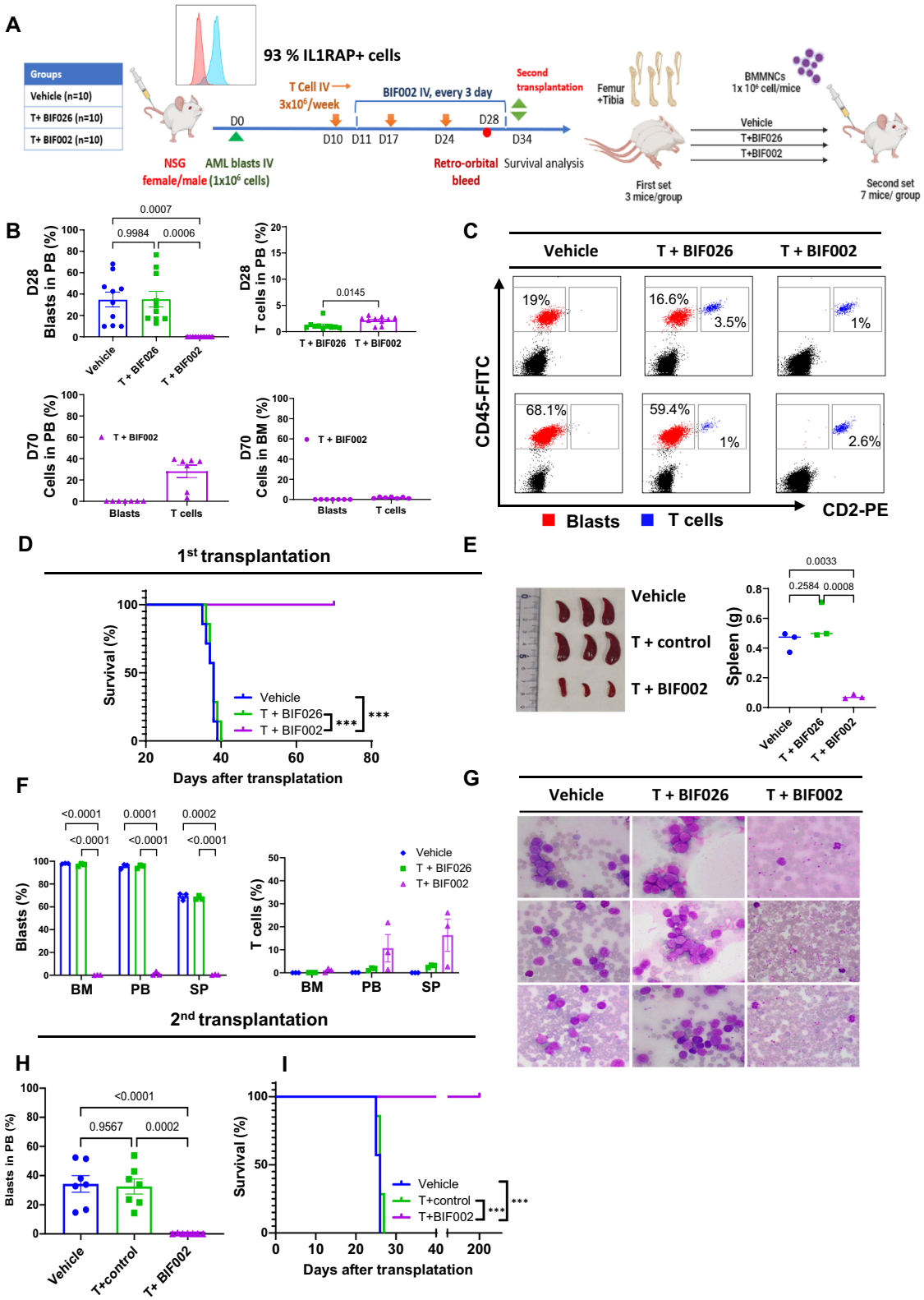

Fig. 7 (See legend on previous page.)

Abbreviations

AML	Acute myeloid leukemia
BiTE	Bispecific T-cell engager
CAR-T	Chimeric antigen receptor T cells
CDR	Complementarity determining regions
ECD	Extracellular domain
FAE	Fab-arm exchange
GFP	Green fluorescent protein
HSC	Hematopoietic stem cells
IEC	Ion exchange chromatography
IL1RAP	The interleukin-1 receptor accessory protein
LSC	Leukemic stem cells
mAbs	Monoclonal antibodies
PDX	Patient derived xenograft
R/R	Refractory/relapsed
RTCA	Real time cell analysis
SEC	Size exclusion chromatography
SPR	Surface plasmon resonance
TCE	T cell engager

Supplementary Information

The online version contains supplementary material available at https://doi.org/10.1186/s13045-024-01586-x.

Additional file1 (DOCX 12366 KB)

Additional file 2 (AVI 16032 KB)

Additional file 3 (AVI 16049 KB)

Acknowledgements
We acknowledge the Antibody Discovery Engine supported by the Integrated Drug Development Venture (IDDV) of City of Hope and funding from IDDV for this project. Special thanks to Drs. Tim Synold and Aparna Krishnan from the Analytical Pharmacology Core for assistance with pharmacokinetics (PK) design, analysis, and interpretation. We also recognize the valuable support of the Animal Resources Center, Hematopoietic Tissue Biorepository, Research Histology/Research Pathology Shared Resource Core, Analytical Cytometry Core, Drug Discovery and Structural Biology Core and Light Microscopy Core at the City of Hope Comprehensive Cancer Center, supported by the National Cancer Institute of the National Institutes of Health under award number P30CA33572. Our appreciation goes to the City of Hope Comprehensive Cancer Center, the patients, and their physicians for contributing primary patient material to this study.

Author contributions
Y.Z. and M.P. designed and conducted the experiments, analyzed the data, designed the figures and wrote the manuscript; L.Y.G. designed experiments, analyzed data, and wrote manuscript; M.P., A.G., K.L., B.P., and H.C. generated, characterized and manufactured the antibodies; E.N., D.D.Z., M.V., X.B.G., L.X.T.N., and J.S. conducted experiments and analyzed data; F.C., H.K, Z.H.C., F.P., J.J.C., S.J.F., and I.A. contributed to experiment design and reviewed data; B.Z., J.J., J.C.W., and G.M. designed experiments, analyzed data, wrote manuscripts, and provided administrative support.

Funding
This research received partial support from National Cancer Institute grants: CA286160 (B.Z. and G.M.), CA258981 (G.M. and B.Z.), CA248475 (G.M. and B.Z.), the MPN Foundation (I.A.), the V Foundation (G.M.), the Robert & Lynda Altman Family Foundation Research Fund and the Natural Science Foundation of China (grant no. 82100159) (Y.Z.).

Declarations

Ethics approval and consent to participate
Human sample acquisition was approved by the City of Hope Institutional Review Board (protocol numbers 18067, 07047 and 06229) at the City of Hope National Medical Center, in accordance with an assurance filed with and approved by the Department of Health and Human Services and met all requirements of the Declaration of Helsinki. Mouse care and experiments were performed in accordance with federal guidelines and under the Institutional Animal Care and Use Committee (IACUC) at the City of Hope approved protocol (#15005).

Consent for publication
Not applicable.

Availability of data and materials
No datasets were generated or analysed during the current study.

Competing interests
Aspects of this work are described and claimed in a pending patent application.

Author details
[1]Department of Hematology, The First Affiliated Hospital, Zhejiang University School of Medicine, Hangzhou, People's Republic of China. [2]Department of Hematologic Malignancies Translational Science, Gehr Family Center for Leukemia Research, Beckman Research Institute, City of Hope, Duarte, CA, USA. [3]Department of Cancer Biology and Molecular Medicine, Beckman Research Institute, City of Hope, Duarte, CA, USA. [4]Department of Clinical Laboratory, The Second Affiliated Hospital, Zhejiang University School of Medicine, Hangzhou, China. [5]Department of Systems Biology, Beckman Research Institute, City of Hope, Duarte, CA, USA. [6]Department of Pathology, City of Hope National Medical Center, Duarte, CA, USA. [7]Department of Hematology and Hematopoietic Cell Transplantation, City of Hope National Medical Center, 1500 E Duarte Road, Duarte, CA 91010, USA.

Received: 7 June 2024 Accepted: 31 July 2024
Published online: 14 August 2024

References

1. DiNardo CD, Erba HP, Freeman SD, Wei AH. Acute myeloid leukaemia. Lancet. 2023;401(10393):2073–86.
2. Shimony S, Stahl M, Stone RM. Acute myeloid leukemia: 2023 update on diagnosis, risk-stratification, and management. Am J Hematol. 2023;98(3):502–26.
3. Liu H. Emerging agents and regimens for AML. J Hematol Oncol. 2021;14(1):49.
4. Kantarjian HM, Kadia TM, DiNardo CD, Welch MA, Ravandi F. Acute myeloid leukemia: treatment and research outlook for 2021 and the MD Anderson approach. Cancer. 2021;127(8):1186–207.
5. Stelmach P, Trumpp A. Leukemic stem cells and therapy resistance in acute myeloid leukemia. Haematologica. 2023;108(2):353–66.
6. Woll PS, Yoshizato T, Hellström-Lindberg E, Fioretos T, Ebert BL, Jacobsen SEW. Targeting stem cells in myelodysplastic syndromes and acute myeloid leukemia. J Intern Med. 2022;292(2):262–77.
7. Vetrie D, Helgason GV, Copland M. The leukaemia stem cell: similarities, differences and clinical prospects in CML and AML. Nat Rev Cancer. 2020;20(3):158–73.
8. Guy DG, Uy GL. Bispecific antibodies for the treatment of acute myeloid leukemia. Curr Hematol Malig Rep. 2018;13(6):417–25.
9. Daver N, Alotaibi AS, Bucklein V, Subklewe M. T-cell-based immunotherapy of acute myeloid leukemia: current concepts and future developments. Leukemia. 2021;35(7):1843–63.
10. Tian Z, Liu M, Zhang Y, Wang X. Bispecific T cell engagers: an emerging therapy for management of hematologic malignancies. J Hematol Oncol. 2021;14(1):75.
11. Aureli A, Marziani B, Sconocchia T, Del Principe MI, Buzzatti E, Pasqualone G, Venditti A, Sconocchia G. Immunotherapy as a turning point in the treatment of acute myeloid leukemia. Cancers. 2021;13(24):1.
12. Aigner M, Feulner J, Schaffer S, Kischel R, Kufer P, Schneider K, Henn A, Rattel B, Friedrich M, Baeuerle PA, et al. T lymphocytes can be effectively recruited for ex vivo and in vivo lysis of AML blasts by a novel CD33/CD3-bispecific BiTE antibody construct. Leukemia. 2013;27(5):1107–15.
13. Chichili GR, Huang L, Li H, Burke S, He L, Tang Q, Jin L, Gorlatov S, Ciccarone V, Chen F, et al. A CD3xCD123 bispecific DART for redirecting host

T cells to myelogenous leukemia: preclinical activity and safety in nonhuman primates. Sci Transl Med. 2015;7(289):289ra282.
14. Bonnevaux H, Guerif S, Albrecht J, Jouannot E, De Gallier T, Beil C, Lange C, Leuschner WD, Schneider M, Lemoine C, et al. Pre-clinical development of a novel CD3-CD123 bispecific T-cell engager using cross-over dual-variable domain (CODV) format for acute myeloid leukemia (AML) treatment. Oncoimmunology. 2021;10(1):1945803.
15. Leong SR, Sukumaran S, Hristopoulos M, Totpal K, Stainton S, Lu E, Wong A, Tam L, Newman R, Vuillemenot BR, et al. An anti-CD3/anti-CLL-1 bispecific antibody for the treatment of acute myeloid leukemia. Blood. 2017;129(5):609–18.
16. van Loo PF, Hangalapura BN, Thordardottir S, Gibbins JD, Veninga H, Hendriks LJA, Kramer A, Roovers RC, Leenders M, de Kruif J, et al. MCLA-117, a CLEC12AxCD3 bispecific antibody targeting a leukaemic stem cell antigen, induces T cell-mediated AML blast lysis. Expert Opin Biol Ther. 2019;19(7):721–33.
17. Yeung YA, Krishnamoorthy V, Dettling D, Sommer C, Poulsen K, Ni I, Pham A, Chen W, Liao-Chan S, Lindquist K, et al. An optimized full-length FLT3/CD3 bispecific antibody demonstrates potent anti-leukemia activity and reversible hematological toxicity. Mol Ther. 2020;28(3):889–900.
18. Mehta NK, Pfluegler M, Meetze K, Li B, Sindel I, Vogt F, Marklin M, Heitmann JS, Kauer J, Osburg L, et al. A novel IgG-based FLT3xCD3 bispecific antibody for the treatment of AML and B-ALL. J Immunother Cancer. 2022;10(3):1.
19. Arruda LCM, Stikvoort A, Lambert M, Jin LQ, Rivera LS, Alves RMP, de Moura TR, Mim C, Lehmann S, Axelsson-Robertson R, et al. A novel CD34-specific T-cell engager efficiently depletes acute myeloid leukemia and leukemic stem cells in vitro and in vivo. Haematologica. 2022;107(8):1786–95.
20. Haubner S, Perna F, Kohnke T, Schmidt C, Berman S, Augsberger C, Schnorfeil FM, Krupka C, Lichtenegger FS, Liu X, et al. Coexpression profile of leukemic stem cell markers for combinatorial targeted therapy in AML. Leukemia. 2019;33(1):64–74.
21. Taussig DC, Pearce DJ, Simpson C, Rohatiner AZ, Lister TA, Kelly G, Luongo JL, Danet-Desnoyers GA, Bonnet D. Hematopoietic stem cells express multiple myeloid markers: implications for the origin and targeted therapy of acute myeloid leukemia. Blood. 2005;106(13):4086–92.
22. Bakker AB, van den Oudenrijn S, Bakker AQ, Feller N, van Meijer M, Bia JA, Jongeneelen MA, Visser TJ, Bijl N, Geuijen CA, et al. C-type lectin-like molecule-1: a novel myeloid cell surface marker associated with acute myeloid leukemia. Cancer Res. 2004;64(22):8443–50.
23. Ma H, Padmanabhan IS, Parmar S, Gong Y. Targeting CLL-1 for acute myeloid leukemia therapy. J Hematol Oncol. 2019;12(1):41.
24. Jaras M, Johnels P, Hansen N, Agerstam H, Tsapogas P, Rissler M, Lassen C, Olofsson T, Bjerrum OW, Richter J, et al. Isolation and killing of candidate chronic myeloid leukemia stem cells by antibody targeting of IL-1 receptor accessory protein. Proc Natl Acad Sci USA. 2010;107(37):16280–5.
25. Agerstam H, Karlsson C, Hansena N, Sanden C, Askmyra M, von Palffy S, Hogberg C, Rissler M, Wunderlich M, Juliusson G, et al. Antibodies targeting human IL1RAP (IL1R3) show therapeutic effects in xenograft models of acute myeloid leukemia. Proc Natl Acad Sci USA. 2015;112(34):10786–91.
26. Boraschi D, Italiani P, Weil S, Martin MU. The family of the interleukin-1 receptors. Immunol Rev. 2018;281(1):197–232.
27. Zarezadeh Mehrabadi A, Aghamohamadi N, Khoshmirsafa M, Aghamajidi A, Pilehforoshha M, Massoumi R, Falak R. The roles of interleukin-1 receptor accessory protein in certain inflammatory conditions. Immunology. 2022;166(1):38–46.
28. Mitchell K, Barreyro L, Todorova TI, Taylor SJ, Antony-Debre I, Narayanagari SR, Carvajal LA, Leite J, Piperdi Z, Pendurti G, et al. IL1RAP potentiates multiple oncogenic signaling pathways in AML. J Exp Med. 2018;215(6):1709–27.
29. Zhang HF, Hughes CS, Li W, He JZ, Surdez D, El-Naggar AM, Cheng H, Prudova A, Delaidelli A, Negri GL, et al. Proteomic screens for suppressors of anoikis identify IL1RAP as a promising surface target in Ewing Sarcoma. Cancer Discov. 2021;11(11):2884–903.
30. Barreyro L, Will B, Bartholdy B, Zhou L, Todorova TI, Stanley RF, Ben-Neriah S, Montagna C, Parekh S, Pellagatti A, et al. Overexpression of IL-1 receptor accessory protein in stem and progenitor cells and outcome correlation in AML and MDS. Blood. 2012;120(6):1290–8.
31. De Boer B, Sheveleva S, Apelt K, Vellenga E, Mulder AB, Huls G, Jacob Schuringa J. The IL1-IL1RAP axis plays an important role in the inflammatory leukemic niche that favors acute myeloid leukemia proliferation over normal hematopoiesis. Haematologica. 2021;106(12):3067–78.
32. Askmyr M, Agerstam H, Hansen N, Gordon S, Arvanitakis A, Rissler M, Juliusson G, Richter J, Jaras M, Fioretos T. Selective killing of candidate AML stem cells by antibody targeting of IL1RAP. Blood. 2013;121(18):3709–13.
33. Landberg N, Hansen N, Askmyr M, Ågerstam H, Lassen C, Rissler M, Hjorth-Hansen H, Mustjoki S, Järås M, Richter J, et al. IL1RAP expression as a measure of leukemic stem cell burden at diagnosis of chronic myeloid leukemia predicts therapy outcome. Leukemia. 2016;30(1):253–7.
34. Zhang B, Chu S, Agarwal P, Campbell VL, Hopcroft L, Jorgensen HG, Lin A, Gaal K, Holyoake TL, Bhatia R. Inhibition of interleukin-1 signaling enhances elimination of tyrosine kinase inhibitor-treated CML stem cells. Blood. 2016;128(23):2671–82.
35. Agerstam H, Hansen N, von Palffy S, Sanden C, Reckzeh K, Karlsson C, Lilljebjorn H, Landberg N, Askmyr M, Hogberg C, et al. IL1RAP antibodies block IL-1-induced expansion of candidate CML stem cells and mediate cell killing in xenograft models. Blood. 2016;128(23):2683–93.
36. Robbrecht D, Jungels C, Sorensen MM, Spanggaard I, Eskens F, Fretland SO, Guren TK, Aftimos P, Liberg D, Svedman C, et al. First-in-human phase 1 dose-escalation study of CAN04, a first-in-class interleukin-1 receptor accessory protein (IL1RAP) antibody in patients with solid tumours. Br J Cancer. 2022;126(7):1010–7.
37. Trad R, Warda W, Alcazer V, Neto da Rocha M, Berceanu A, Nicod C, Haderbache R, Roussel X, Desbrosses Y, Daguindau E, et al. Chimeric antigen receptor T-cells targeting IL-1RAP: a promising new cellular immunotherapy to treat acute myeloid leukemia. J Immunother Cancer. 2022;10(7):1.
38. Warda W, Larosa F, Neto Da Rocha M, Trad R, Deconinck E, Fajloun Z, Faure C, Caillot D, Moldovan M, Valmary-Degano S, et al. CML hematopoietic stem cells expressing IL1RAP can be targeted by chimeric antigen receptor-engineered T cells. Cancer Res. 2019;79(3):663–75.
39. Labrijn AF, Meesters JI, Priem P, de Jong RN, van den Bremer ET, van Kampen MD, Gerritsen AF, Schuurman J, Parren PW. Controlled Fab-arm exchange for the generation of stable bispecific IgG1. Nat Protoc. 2014;9(10):2450–63.
40. Liu L, Jacobsen FW, Everds N, Zhuang Y, Yu YB, Li N, Clark D, Nguyen MP, Fort M, Narayanan P, et al. Biological characterization of a stable effector functionless (SEFL) monoclonal antibody scaffold in vitro. J Biol Chem. 2017;292(5):1876–83.
41. Han L, Dong L, Leung K, Zhao Z, Li Y, Gao L, Chen Z, Xue J, Qing Y, Li W, et al. METTL16 drives leukemogenesis and leukemia stem cell self-renewal by reprogramming BCAA metabolism. Cell Stem Cell. 2023;30(1):52-68.e13.
42. Frenay J, Bellaye PS, Oudot A, Helbling A, Petitot C, Ferrand C, Collin B, Dias AMM. IL-1RAP, a key therapeutic target in cancer. Int J Mol Sci. 2022;23(23):1.
43. Zhang Y, Chen X, Wang H, Gordon-Mitchell S, Sahu S, Bhagat TD, Choudhary G, Aluri S, Pradhan K, Sahu P, et al. Innate immune mediator, Interleukin-1 receptor accessory protein (IL1RAP), is expressed and protumorigenic in pancreatic cancer. J Hematol Oncol. 2022;15(1):70.
44. Rydberg Millrud C, Deronic A, Gronberg C, Jaensson Gyllenback E, von Wachenfeldt K, Forsberg G, Liberg D. Blockade of IL-1alpha and IL-1beta signaling by the anti-IL1RAP antibody nadunolimab (CAN04) mediates synergistic anti-tumor efficacy with chemotherapy. Cancer Immunol Immunother. 2023;72(3):667–78.

Publisher's Note